Study of microparticles incorporation in coatings on titanium produced by plasma electrolytic oxidation (PEO)

F. Ceriani, L. Casanova, M.V. Diamanti, M. Ormellese, M. Pedeferri

This research is focused on the analysis of the influence of rutile (TiO_2) and anatase (TiO_2) microparticles (d < 5 μm) on the morphology, structure, and anticorrosive properties of PEO coatings on titanium produced in alkaline based solution containing sodium hydroxide and sodium metasilicates or nanoclay particles (hydrophilic bentonite, $H_2Al_2O_6Si$, d < 25 μm).

PEO coatings are characterized by scanning electron microscope (SEM), energy dispersive spectroscopy (EDS) and X-ray diffraction (XRD). In addition, the samples are electrochemically investigated by electrochemical impedance spectroscopy analysis.

The tests carried out have shown that the incorporation of TiO_2 microparticles in the coating leads to the formation of thick oxide layers characterized by a fine porosity. These coatings provide good corrosion protection when samples are exposed to an aggressive sulfuric acid solution.

KEYWORDS: CORROSION, TITANIUM, PEO, EIS, MICROPARTICLES

INTRODUCTION

Plasma electrolytic oxidation (PEO) is an electrochemical surface treatment designed to produce a thick and hard oxide layer on the surface of the treated metal, typically titanium, aluminum or magnesium. The metal component is immersed in a suitable electrolytic solution and is connected to a voltage source applied between the metal (the anode) and a counter electrode. The high voltages can allow to overcome the breakdown potential of the oxide with consequent generation of plasma. [1]

The ceramic coating thus obtained is characterized by the presence of pores, produced by the discharges and by the aggressive environment to which the component is exposed during the PEO process. These defects could cause a reduction in the corrosion resistance of the treated component, favoring the transport of aggressive ions through the oxide. [2] To solve this problem, a viable option is represented by the addition of solid particles to the electrolytic solution used for the PEO treatment to favor the formation of a less porous structure thanks to the filling effect of the pores by the particles embedded within the forming oxide. [2], [3] Among the various types of particles that can be used, those of metal

F. Ceriani, L. Casanova, M.V. Diamanti, M. Ormellese, M. Pedeferri
Dept. of Chemistry, Materials and Chemical Engineering "G. Natta", Politecnico di Milano, Via Mancinelli 7, 20131 Milano, Italy

oxides are particularly effective for improving corrosion resistance, such as, for example, titanium dioxide (TiO_2) particles which, in addition to enhance the anti-corrosion performance of PEO oxides, increase their hardness and wear resistance. [4] The aim of this study is to verify the effect of the incorporation of TiO_2 microparticles on the corrosion resistance of PEO coatings for applications in the chemical field.

MATERIALS AND METHODS

The PEO process is performed using a commercial potentiostat, connecting the sample to be anodized to the positive pole. A cylindrical activated titanium mesh is used as a counter electrode. The applied signal consists of a 60% anodic and 40% cathodic waveform, with a cathodic peak equal to 7% of the anodic one, supplied at a frequency of 1000 Hz. The applied potential increases linearly from 0 V to 90 V via a ramp of 320 s. The treatment is performed on 10 x 10 x 1.2 mm^3 samples of Ti grade 2 obtained by metal shearing, polished with silicon carbide paper (120-600 mesh) and rinsed with distilled water. The electrolyte used consists of an aqueous solution of 1 M NaOH to which microparticles (≤ 5 μm) of rutile or anatase are added. From this base solution, four different electrolytes are obtained by adding sodium metasilicates (Na_2SiO_3) and nanoclay (hydrophilic bentonite, $H_2Al_2O_6Si$, ≤ 25 μm). Both additives contain Si which favors the formation of a more stable and compact oxide. [5] The compositions of the solutions are shown in Table 1.

Tab.1 - Compositions of the used electrolytic solutions (R = rutile, A = anatase, S = silicates, C = nanoclay)

LABELS	BASE SOLUTION	ADDITIVES
R_S	1 M NaOH	5 $g \cdot L^{-1}$ R + 4 $g \cdot L^{-1}$ Na_2SiO_3
A_S		5 $g \cdot L^{-1}$ A + 4 $g \cdot L^{-1}$ Na_2SiO_3
R_C		5 $g \cdot L^{-1}$ R + 15 $g \cdot L^{-1}$ nanoclay
A_C		5 $g \cdot L^{-1}$ A+ 15 $g \cdot L^{-1}$ nanoclay
Ti_Na		-

The PEO process is carried out in a 1 L beaker containing 500 mL of solution kept under agitation using a magnetic stirrer at a speed of 600 rpm to promote homogeneous dispersion of the particles.

The characterization of PEO coatings occurs via scanning electron microscopy (SEM) for which a microscope equipped with an energy dispersive spectroscopy (EDS) spectrometer is used. The crystalline structure of the oxides is evaluated by X-ray diffraction performed using a goniometer with Cu Kα1 radiation (1.54058 Å). Finally, electrochemical impedance spectroscopy (EIS) analyses are carried out in 10% v/v sulfuric acid solution maintained at 60 °C. This solution aims to reproduce the aggressive conditions that can be encountered in some chemical treatments of metals, for example during pickling operations. The EIS tests are carried out with a potentiostat/galvanostat using a standard three-electrode cell with a volume of 250 ml, in which the reference electrode is a saturated silver/silver chloride (SSC) electrode and the counter electrode is a platinum electrode. The measurements are carried out in a frequency window $10^5 \div 10^{-2}$ Hz, applying a sinusoidal signal of 10 mV_{rms} and analyzing 10 points per decade of frequency.

RESULTS AND DISCUSSION

SEM Analyses

The SEM images of the surfaces of the four samples (Fig. 1 a), show the presence of rounded protuberances often surmounted by pores. The formation of these structures is due to the effect of the pressure exerted on the molten oxide by the gases (oxygen, hydrogen, steam) trapped inside the coating during the growth phase. When cooling and solidification of the oxide begin, the gas is sometimes evacuated, generating pores. [6], [7]

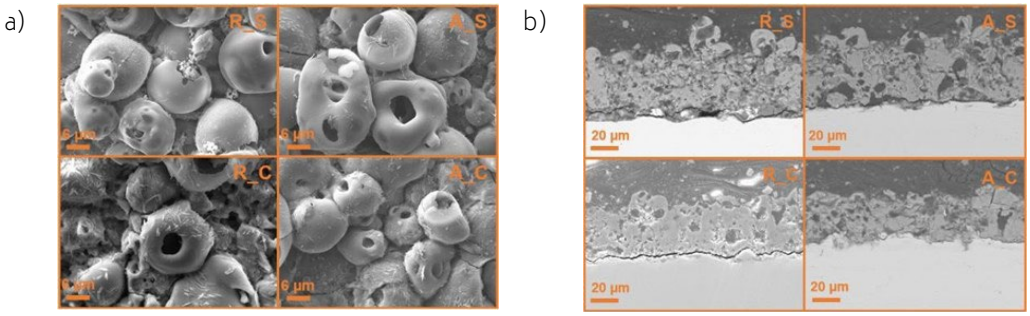

Fig. 1 - a) SEM images of the surfaces of PEO samples; b) SEM images of the cross-sections of PEO samples.

The analysis of the sections of the coatings using SEM (Fig. 1 b) allows to estimate the thickness of the oxides. By working with rutile particles, coatings with thicknesses of approximately 52 µm (R_S) and 35 µm (R_C) are reached, in the presence of silicates and nanoclay respectively. As regards the samples treated with anatase, thicknesses of approximately 49 µm (A_S) using silicates and 30 µm (A_C) in the presence of nanoclay are obtained.

It could be noted that the greater thicknesses are achieved by working with metasilicates in addition to the microparticles: this phenomenon is the result of a double effect, i.e. the stabilization effect of the SiO_3^{2-} ions, which reduces the dissolution of the oxide in solution favoring its growth, and their polymerization. [5]

Another important observation concerns the structure of the oxides, it is observed that while the coatings produced in electrolytes containing rutile have a fine and uniform porosity, the oxides obtained by working with anatase microparticles are characterized by larger pores. These large defects may compromise the corrosion protection effect as they allow the penetration of the aggressive solution through the oxide. Coatings produced in the presence of rutile particles are instead characterized by the presence of cracks at the interface between the substrate and the oxide itself; this defect could potentially compromise the adhesion of the coating to the substrate.

The EDS analyses (not reported) allow to verify the presence of Ti, O, Na and Si in all the samples. Furthermore, in the coatings produced using nanoclay, the presence of Al is also detected. These results permit to confirm the effective participation of the additives of the electrolytic solution in the plasma events typical of PEO anodization and their incorporation into the produced oxides.

XRD Analyses

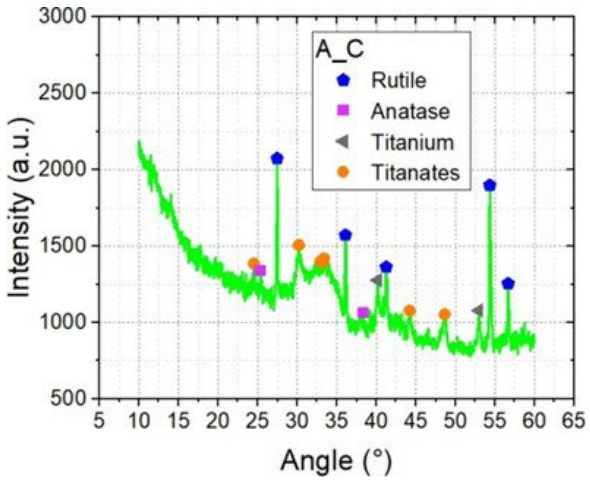

Fig. 2 - XRD graph of the A_C sample.

The XRD analyses of the samples (A_C diffractogram is shown in Fig. 2 for exemplary purposes) confirmed the presence of rutile in all coatings. The most intense signal in the diffractogram always corresponds to this crystalline structure, even in samples treated with anatase, suggesting a partial transformation of anatase into rutile favored by

the high temperatures reached during plasma events. [8] The anatase peaks, instead, are observed only for the oxides produced in the presence of these microparticles. All specimens show peaks related to metallic titanium, whose intensity decreases according to the thickness of the coating. This hypothesis seems to be confirmed by considering the oxide thicknesses evaluated through the analysis of the SEM images of the sample cross-sections. The oxides produced using nanoclay are characterized by the lowest thicknesses and the most intense Ti signals.

Another feature common to all diffractograms is the broad peak produced at 30÷35° which reveals the presence of SiO_2 in the amorphous phase. [9] This data provides further confirmation of the incorporation of silicon-based additives within the coatings. Finally, peaks associated with sodium titanates, $Na_2Ti_6O_{13}$, produced by the reaction between titanium dioxide and sodium hydroxide are detected in the samples treated with nanoclay. [10]

EIS Analyses

The results of the electrochemical impedance tests are shown in Fig. 3, where the Nyquist curves representing the first and sixth cycles of a series of measurements conducted over 1 hour and 30 minutes are depicted. The EIS measurements are carried out after 30 minutes of monitoring of the free corrosion potential. During the entire duration of the test the samples remained immersed in the sulfuric acid solution.

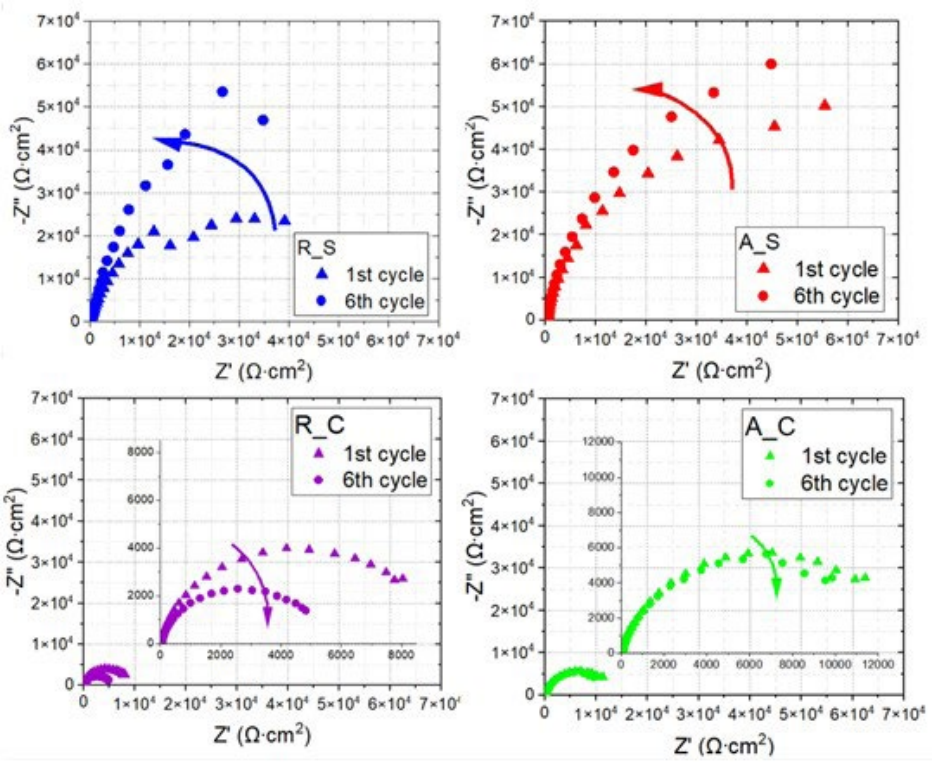

Fig. 3 - Nyquist diagrams of PEO samples.

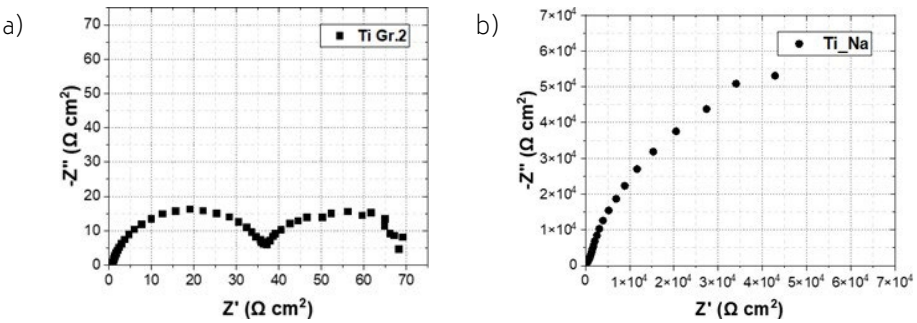

Fig. 4 - Nyquist diagram a) of Ti grade 2, and b) of Ti treated without MPs after 30 minutes of immersion.

Comparing the results of the impedance tests obtained for the PEO specimens with those of the untreated Ti grade 2 (Fig. 4. a), it is observed that the behavior of the samples changes significantly. The Nyquist diagram of bare Ti presents a double semicircle typical of a corrosive process and a polarization resistance, R_p (defined as the intersection of the arcs that interpolate the Nyquist graphs with the axis of the real impedance Z') typical of an active electrode (about 70 Ω cm^2). [11] The specimens coated with PEO oxides, instead, show only one capacitive semicircle and R_p values that are four and five orders of magnitude higher for the samples treated with nanoclays and metasilicates, respectively, compared to Ti grade 2. These values demonstrate the corrosion protection ability of PEO coatings.

Looking in more detail at the graphs relating to PEO coatings (Fig. 3) it is immediately possible to notice an important difference between the oxides produced using the two different types of Si-containing additives.

First of all, the impedance curves of the samples treated with nanoclay are semicircles with reduced diameter, an indication of a low polarization resistance which for the R_C and A_C samples is lower than 15000 Ω·cm^2. Such values are lower than the R_p of the Ti treated under the same conditions described in the Materials and Methods section, but in the absence of particles (Fig. 4. b, R_p of approximately 120000 Ω·cm^2). Concerning the samples prepared with solutions containing silicates, instead, arcs with larger diameters and R_p in the order of 150000 Ω·cm2 are observed (an order of magnitude higher than the values indicated for R_C and A_C and higher than the R_p value of the sample Ti_Na). This difference between the R_p values can be partly justified by the difference in thickness between the two types of coatings. As previously observed, the R_S and A_S oxides have a thickness approximately 20 μm greater than the corresponding coatings produced with nanoclay; this improves the barrier effect of the coatings by making the penetration of aggressive ions slower and consequently increasing the values of R_p. Furthermore, by studying the temporal evolution of the impedance values it can be noted that in the case of R_C and A_C the diameters of the semicircles, and therefore the R_p values, decrease. On the contrary, the impedance values of R_S and A_S increase during the immersion period in the acid solution. This trend may be associated with the formation of corrosion products that fill the pores of the coating, improving its corrosion protection effect.

Finally, it is noted that the impedance values achieved by A_S and A_C are slightly higher than those obtained by their respective rutile-containing counterparts. This phenomenon is probably due to the lower crystallinity of the samples produced through the incorporation of anatase particles, which therefore provide greater resistance to the passage of electrons generating higher impedances. However, it has been widely demonstrated that rutile guarantees better behavior against acid corrosion in long-term tests. [12]

By observing the trend of the imaginary impedance, it is possible to evaluate the kinetics of the ongoing relaxation phenomena. The diagrams obtained (not shown) present a single time constant at low frequencies therefore attributable to a corrosion reaction controlled by the diffusion of aggressive species through the coating. [13]

CONCLUSIONS

This paper describes the effects of adding microparticles to electrolytic solutions used for PEO treatments on titanium.

It is observed that in general, the incorporation of TiO_2 microparticles in coatings allows to generate thick oxides, in particular when the particles are combined with metasilicates, and with R_p values at least four orders of magnitude greater than uncoated Ti grade 2.

By working with rutile and metasilicate microparticles it is possible to produce oxides with a fine and uniform porosity offering a particularly favorable structure in terms of protecting the metal substrate from corrosion since the penetration of aggressive species through the ceramic layer is made more difficult. As regards the oxides obtained in the presence of anatase and metasilicates, although they are characterized by larger pores, they still provide high polarization resistance values, thus guaranteeing excellent resistance to charge flow and good protective behavior. When nanoclay particles are added to the electrolytic solution, thin oxides with high porosity are obtained. Consequently, the coatings are characterized by reduced polarization resistance values and provide lower corrosion protection than oxides produced in the absence of microparticles.

BIBLIOGRAPHY

[1] S. Sikdar, P. V. Menezes, R. Maccione, T. Jacob, and P. L. Menezes, "Plasma electrolytic oxidation (PEO) process—processing, properties, and applications," Nanomaterials, vol. 11, no. 6, 2021, doi: 10.3390/nano11061375.

[2] X. Lu, C. Blawert, M. L. Zheludkevich, and K. U. Kainer, "Insights into plasma electrolytic oxidation treatment with particle addition," Corros. Sci., vol. 101, pp. 201–207, 2015, doi: 10.1016/j.corsci.2015.09.016.

[3] A. Fattah-alhosseini, M. Molaei, and K. Babaei, "The effects of nano- and micro-particles on properties of plasma electrolytic oxidation (PEO) coatings applied on titanium substrates: A review," Surfaces and Interfaces, vol. 21, no. December 2019, p. 100659, 2020, doi: 10.1016/j.surfin.2020.100659.

[4] X. Lu et al., "Plasma electrolytic oxidation coatings with particle additions – A review," Surf. Coatings Technol., vol. 307, pp. 1165–1182, 2016, doi: 10.1016/j.surfcoat.2016.08.055.

[5] S. Moon and Y. Jeong, "Generation mechanism of microdischarges during plasma electrolytic oxidation of Al in aqueous solutions," Corros. Sci., vol. 51, no. 7, pp. 1506–1512, 2009, doi: 10.1016/j.corsci.2008.10.039.

[6] X. Zhang et al., "X-ray Computed Tomographic Investigation of the Porosity and Morphology of Plasma Electrolytic Oxidation Coatings," ACS Appl. Mater. Interfaces, vol. 8, no. 13, pp. 8801–8810, 2016, doi: 10.1021/acsami.6b00274.

[7] E. Matykina, A. Berkani, P. Skeldon, and G. E. Thompson, "Real-time imaging of coating growth during plasma electrolytic oxidation of titanium," Electrochim. Acta, vol. 53, no. 4, pp. 1987–1994, 2007, doi: 10.1016/j.electacta.2007.08.074.

[8] D. A. H. Hanaor and C. C. Sorrell, "Review of the anatase to rutile phase transformation," J. Mater. Sci., vol. 46, no. 4, pp. 855–874, 2011, doi: 10.1007/s10853-010-5113-0.

[9] S. Aliasghari, P. Skeleton, and G. E. Thompson, "Plasma electrolytic oxidation of titanium in a phosphate/silicate electrolyte and tribological performance of the coatings," Appl. Surf. Sci., vol. 316, no. 1, pp. 463–476, 2014, doi: 10.1016/j.apsusc.2014.08.037.

[10] X. Chen and S. S. Mao, "Titanium dioxide nanomaterials: Synthesis, properties, modifications and applications," Chem. Rev., vol. 107, no. 7, pp. 2891–2959, 2007, doi: 10.1021/cr0500535.

[11] L. Casanova, M. La Padula, M. P. Pedeferri, M. V. Diamanti, and M. Ormellese, "An insight into the evolution of corrosion resistant coatings on titanium during bipolar plasma electrolytic oxidation in sulfuric acid," Electrochim. Acta, vol. 379, p. 138190, 2021, doi: 10.1016/j.electacta.2021.138190.

[12] L. Casanova, M. Arosio, M. T. Hashemi, M. Pedeferri, G. A. Botton, and M. Ormellese, "Influence of stoichiometry on the corrosion response of titanium oxide coatings produced by plasma electrolytic oxidation," Corros. Sci., vol. 203, no. January, p. 110361, 2022, doi: 10.1016/j.corsci.2022.110361.

[13] L. Casanova, F. Ceriani, M. Pedeferri, and M. Ormellese, "Addition of Organic Acids during PEO of Titanium in Alkaline Solution," Coatings, vol. 12, no. 2, 2022, doi: 10.3390/coatings12020143.

TORNA ALL'INDICE >